Journal of Polymer Research (2020) 27: 45
https://doi.org/10.1007/s10965-020-2019-7

ORIGINAL PAPER

Chitosan polymer electrolytes doped with a dysprosium ionic liquid

R. Leones [1,2] · P. M. Reis [3] · R. C. Sabadini [4] · J. M. S. S. Esperança [3] · A. Pawlicka [4] · M. M. Silva [1]

Received: 30 September 2019 / Accepted: 29 January 2020 / Published online: 4 February 2020

Abstract

In this work, we studied polymer electrolytes (PEs) that had the natural polymer chitosan as their matrix host. Different quantities of an ionic liquid that contains the lanthanide dysprosium as part of the anion, were incorporated in the chitosan matrix through the solvent casting method. The thermal, morphological and electrochemical properties of the membranes were accessed. The results, obtained by thermogravimetric analysis (TGA), differential scanning calorimetry (DSC), X-ray diffraction (XRD), scanning electron microscopy (SEM), force microscopy (AFM), and complex impedance spectroscopy, revealed a minimum thermal stability of about 139 °C; a predominantly amorphous morphology combined with the presence of small crystalline domains and a satisfactory ionic conductivity. The sample with the highest ionic conductivity was the chitosan$_1$[C_2mim][Dy(SCN)$_4$], (where 1 corresponds to the quotient between the mass of the polymer and the mass of the IL) which attained 6.76×10^{-6} S·cm^{-1} at 30 °C and 5.62×10^{-4} S·cm^{-1} at 100 °C. The results presented here suggest that these materials are promising and may find application in practical electrochemical devices.

Keywords Dysprosium · Polymer electrolytes · Ionic liquid · Chitosan · Natural polymer · Ionic conductivity

Introduction

In general, ionic liquids (ILs) have distinguishing properties, such as almost negligible vapor pressures, high thermal stabilities, wide liquid ranges, considerable conductivities, and large electrochemical windows [1–5]. Such characteristics have proved to be valuable for a great deal of applications. Additionally, as ILs are composed of distinct cations and anions, they are widely tunable, allowing their design for specific applications through the proper choice of both cation and anion [5, 6].

Metal-containing ILs are promising new materials that can combine the properties of ILs with magnetic, catalytic or photophysical/optical properties, which are originated from the incorporated metal. Recently, it has been shown that solutions of lanthanide compounds in ILs are promising soft luminescent materials for use in photochemistry and spectroscopy [7, 8]. In that sense, our goal was to synthesize an IL that combined both the conductivity of ILs with the luminescence of lanthanide complexes. For this purpose, a dysprosium-based IL was synthesized and incorporated in chitosan polymer electrolytes (PEs) membranes.

PEs are very appealing ionically conducting materials that can find application in solid-state electrochemical devices, such as rechargeable batteries, electrochromic displays, capacitors or sensors [9, 10]. Because of its extraordinary solvating ability toward salts, poly(oxyethylene) (POE) has been the macromolecule most widely used to produce PEs [11]. Nevertheless, technological progress and environmental concerns push towards new PEs materials with unique properties. Recently, new PEs based on natural polymers have been successfully proposed [12–29].

Natural polymers like chitosan, gelatin, agar-agar, pectin, cellulose or starch offer sought after advantages such as biodegradability, low production cost and inexhaustible sources [12–14]. In this work we explored the preparation and characterization of PEs membranes based on chitosan. Chitosan is a linear

✉ M. M. Silva
nini@quimica.uminho.pt

1 Centro de Química, Universidade do Minho, Campus de Gualtar, 4710-057 Braga, Portugal

2 Leibniz IFW Dresden, Helmholtzstr. 20, 01069 Dresden, Germany

3 LAQV, REQUIMTE, Departamento de Química, Faculdade de Ciências e Tecnologia, Universidade Nova de Lisboa, 2829-516 Caparica, Portugal

4 Instituto de Química de São Carlos, Universidade de São Paulo, São Carlos, SP 13566-590, Brazil

copolymer of β-(1–4) linked glucosamine and N-acetylglucosamine, that can be found in fungi, insects and crustacean shells [30–33]. It is broadly used in the food packaging, pharmaceutical and biomedical industries and its physical and chemical properties depend on its degree of acetylation, intramolecular residues distribution and molecular weight [30–35]. Chitosan's polar functional groups foment its ability to dissolve ionic salts, which is a vital feature for a PE matrix host [36–38].

The present work is focused on the synthesis of a dysprosium-based IL, its incorporation in chitosan PEs membranes and their respective characterization. The PEs thermal, morphological and electrochemical characterization was attained through thermogravimetric analysis (TGA), differential scanning calorimetry (DSC), X-ray diffraction (XRD), scanning electron microscopy (SEM), force microscopy (AFM), and complex impedance spectroscopy.

Materials and methods

Synthesis of $[C_2mim][Dy(SCN)_4]\cdot 3(H_2O)$

The synthesis of $[C_2mim][Dy(SCN)_4].3H_2O$ is described by eqs. 1–3.

$$2\ NaSCN + H_2SO_4 \rightarrow Na_2SO_4\downarrow + 2\ HSCN \quad (1)$$

$$6\ HSCN + Dy_2O_3 \rightarrow 2Dy(SCN)_3.3H_2O \quad (2)$$

$$Dy(SCN)_3.3H_2O + [C_2mim][SCN] \rightarrow [C_2mim]\left[Dy(SCN)_4\right].3H_2O \quad (3)$$

NaSCN (6.48 g, 80 mmol) (Fluka, > 98%) was dissolved in Milli-Q water (25 mL). The addition of H_2SO_4 (2.2 mL, 40 mmol) (Merck, 96%) to this solution produced a mixture of HSCN and Na_2SO_4. To enable Na_2SO_4 precipitation, 50 mL of ethanol (Carlo Erba Reagents, 99.9%) were added. The precipitate was removed by filtration. Dy_2O_3 (4.48 g, 12 mmol) (Alfa Aesar, 99.9%) was added to the obtained filtrate (an aqueous solution with circa 80 mmol HSCN) and the heterogeneous mixture was left under stirring overnight. The reaction mixture containing $Dy(SCN)_3.3H_2O$ was evaporated in a rotavapor and dried in a vacuum line (10^{-3} bar) [39].

A mixture of $Dy(SCN)_3.3H_2O$ (2.0417 g, 4.78 mmol) and $[C_2mim][SCN]$ (0.810 g, 4.78 mmol) (Iolitec, > 98%) was stirred for 2 h at 120 °C, following a similar procedure [40]. The mixture containing the desired IL, $[C_2mim][Dy(SCN)_4].3H_2O$, was dried under vacuum, yielding an orange solid.

NMR could not be used as a characterization technique due to the paramagnetic properties of this IL.

Elemental analysis was used to evaluate the resulting orange solid. The results confirmed the production of the dysprosium-based IL $[C_2mim][Dy(SCN)_4].3H_2O$.

Calculated: % C: 21.45; % N: 15.01; % H: 3.06.
Measured: % C: 21.40; % N: 15.24; % H: 2.77.

PEs preparation

Chitosan (0.2 g) (medium molecular weight and 75–85% deacetylated, Sigma-Aldrich 448,877) was dissolved in a 1% acetic acid solution (10 mL) (Sigma-Aldrich, > 99.8%) and stirred overnight at room temperature. Then, different quantities of the IL (0.05–0.4 g) and glycerol (0.2 g) (Himedia, 99.5%) were added. The obtained homogeneous and viscous solution was poured onto Petri dishes and dried under a temperature gradient (5 h at 25 °C, then 12 h at 40 °C, followed by 5 h at 60 °C and then cooled down to 25 °C for 2 h). The resulting flexible transparent membranes thickness ranged from 0.096 to 0.153 ± 0.001 mm. The notation adopted throughout this work was $chitosan_n[C_2mim][Dy(SCN)_4]$, where n corresponds to the quotient between the mass of the polymer and the mass of the IL.

PEs characterization

The thermal behavior of the PEs was studied by TGA and DSC. For the DSC experiments, 40 μL aluminum crucibles with perforated lids were sealed with each sample inside a glove box filled with dry argon. The analyses were carried out using a Mettler DSC 821e under a flowing argon atmosphere in the temperature range – 60 to 140 °C and at a heating rate of 5 $°C \cdot min^{-1}$. TGA analyses were performed with a Shimadzu TGA-50 equipment. The measurements were conducted between 30 and 900 °C, at a heating rate of 10 $°C \cdot min^{-1}$, under a nitrogen atmosphere with a 60 $mL \cdot min^{-1}$ flow rate. Before each analysis and aiming to eliminate the traces of any absorbed moisture, all samples were subject to a first run from 30 to 105 °C, at a heating rate of 20 $°C \cdot min^{-1}$, followed by a second isothermal run at 105 °C for 10 min.

XRD measurements were performed at room temperature with X-ray Rigaku Utma 4 diffractometer, operating with a power of 50 kV/50 mA, Cu Kα irradiation, a speed of 2 $^{o} \cdot min^{-1}$, and an angle range (2θ) from 3 to 60 °.

SEM images were obtained at 10 kV with a LEO 440 microscope.

AFM images were obtained with a Bruker AFM System (Dimension icon with scan Asyst). In all AFM analyses the intermittent-contact mode was employed by using silicon AFM probes with a force constant of 48 $N \cdot m^{-1}$ and a resonance frequency of 190 kHz.

The bulk ionic conductivities of the PEs were measured using an Autolab PGSTAT-12 (Eco Chemie) and the complex plane impedance technique on a cell GE/polymer electrolyte/GE (GE – ion-blocking gold electrode of 10 mm diameter; Goodfellow, > 99.95%). The cell was secured in a suitable constant volume support. The analyses were performed from

room temperature (~20 °C) to 100 °C and over the frequency range from 65 kHz to 500mHz.

Results and discussion

The TGA curves of the chitosan matrix, chitosan$_n$[C_2mim][Dy(SCN)$_4$] membranes and [C_2mim][Dy(SCN)$_4$] (Fig. 1) reveal that the decomposition temperature of the PEs membranes increases with the addition of the IL. The decomposition temperatures ranged from 135 °C, for the chitosan matrix, to about 170 °C, for the chitosan$_{0.5}$[C_2mim][Dy(SCN)$_4$] membrane and pure IL. These results show an IL-stabilizing effect and indicate a thermal degradation influenced mostly by the polymeric matrix. The decomposition temperatures obtained are considered acceptable for most of the envisaged practical applications and comparable to other results in the literature [29].

The thermal properties of these materials were also accessed through DSC (Fig. 2). The absence of any thermal process below 165 °C is consistent with a predominantly amorphous morphology. Above this temperature occurs the thermal degradation of the membranes. The amorphous nature of these electrolytes provides a clear advantage, as the absence of crystallinity is associated with better mechanical, optical and electrochemical behavior [41].

The essentially amorphous nature was confirmed by the XRD results (Fig. 3), as indicated by the Gaussian shaped broad band, centered at around 20.5–22.0 °. A peak analogous to the ones observed for other PEs based on natural macromolecules [42]. Nevertheless, the samples with $n = 4$ and 0.5 depict peaks at around 10, and 33 °. Also, two weaker peaks are detected at around 21 and 25 °for $n = 0.5$, and one peak around 29° for n = 4, suggesting that these peaks are IL-related and

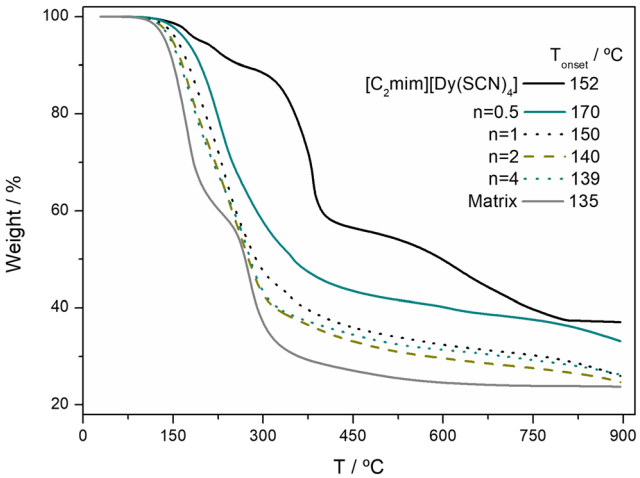

Fig. 1 TGA curves of the chitosan matrix, chitosan$_n$[C_2mim][Dy(SCN)$_4$] membranes and [C_2mim][Dy(SCN)$_4$], and respective onset degradation temperatures

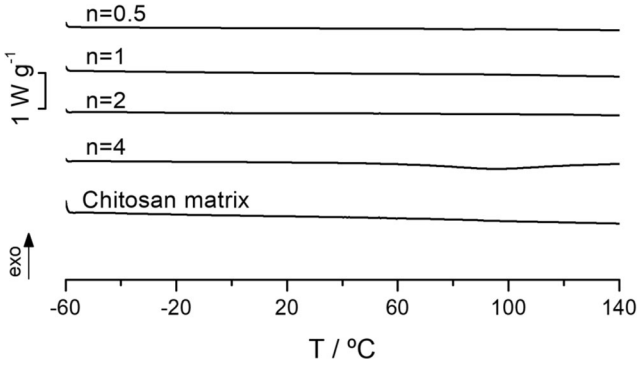

Fig. 2 DSC thermograms of the chitosan matrix and chitosan$_n$[C_2mim][Dy(SCN)$_4$] membranes

similar results were found previously [29]. Such results suggest the formation of a smaller proportion of crystalline domains, though the polymeric chains are predominantly in a disordered orientation. More specifically, these peaks might be linked directly to dysprosium, since similar results were found for other PEs based on chitosan and the salt dysprosium triflate [43].

When the polymer host is unable to accommodate the IL, the recombination of ions can be observed and the crystalline peaks may be attributed to the IL out of the films surface. These chitosan-IL peaks (around 10 and 33° for $n = 0.5$ and $n = 4$) appear at higher 2θ angles, when compared to the peaks of pure IL which is an indication that some long-range order was obtained due to the formation of polymer-IL complexes. [43].

The increase of intensity of peak around, 10° for $n = 0.5$, indicates an increase of the local crystallinity. This increase, which is probably associated with the formation of clusters of IL or polymer-IL complexes, might also suggest that the sample with n = 0.5 reached the maximum capacity of the host matrix to dissolve IL.

The SEM images (Fig. 4) confirm the presence of dysprosium clusters, as suggested by the XRD results. The membrane

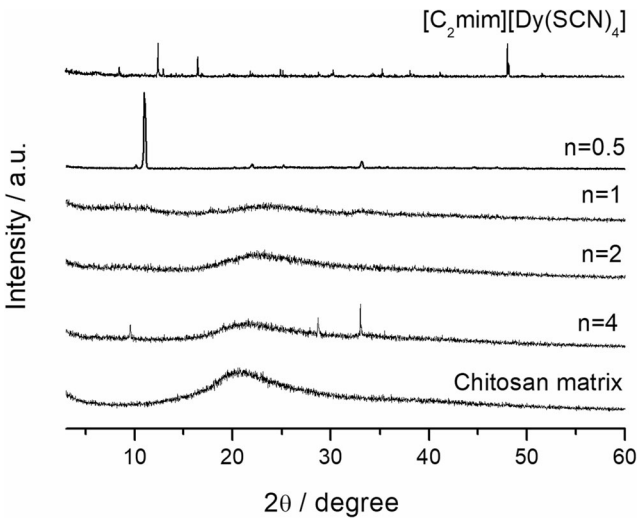

Fig. 3 XRD patterns of the chitosan matrix, chitosan$_n$[C_2mim][Dy(SCN)$_4$] membranes and [C_2mim][Dy(SCN)$_4$]

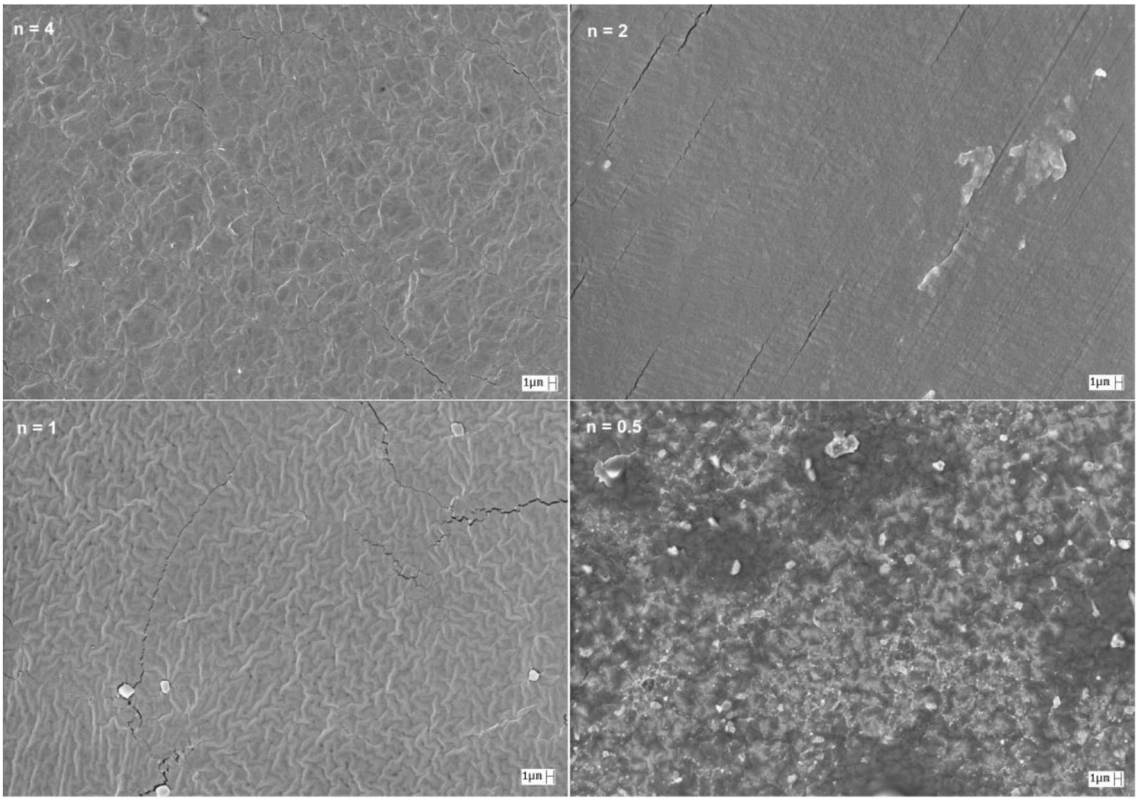

Fig. 4 SEM images of the chitosan$_n$[C_2mim][Dy(SCN)$_4$] membranes

with the highest amount of IL, n = 0.5, is the one that exhibits a more irregular surface, while the remaining samples show smaller and sparser crystalline regions. Besides these irregularities no other phase separation is observed.

The surface morphology of the samples was also examined through AFM. The images of the chitosan$_n$[C_2mim][Dy(SCN)$_4$] membranes were acquired with a scanning area of 5.0 μm × 5.0 μm, while the AFM image of the chitosan matrix was acquired with a scanning area of 10.0 μm × 10.0 μm. Table 1 lists the roughness mean square (RMS) values of the analyzed membranes. The RMS values ranged from 11.1 to 20.4 nm. The sample with the highest surface roughness showed the lowest ionic conductivity, which may be explained by the association of the surface roughness to crystalline domains; the sample with the second lowest surface roughness showed the highest ionic conductivity.

Regarding these materials' luminescence, no signal was observed because the absorption bands of the polymer masked the dysprosium bands. Nevertheless, though these samples do not combine ionic conductivity with luminescence, they do show satisfactory ionic conductivity values. Figure 5 depicts the plot of the temperature dependence of the ionic conductivity of the chitosan matrix and the chitosan$_n$[C_2mim][Dy(SCN)$_4$] membranes.

Table 1 RMS values of the chitosan matrix and the chitosan$_n$[C_2mim][Dy(SCN)$_4$] membranes

	RMS (nm)
Matrix	11.9
n = 4	11.1
n = 2	19.5
n = 1	16.1
n = 0.5	20.4

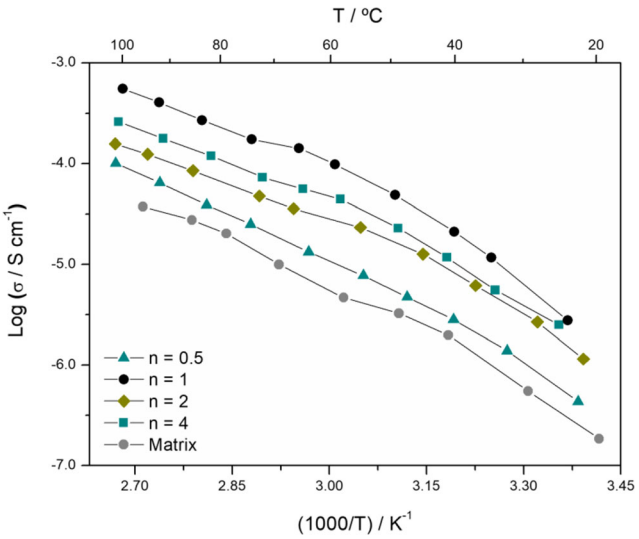

Fig. 5 Variation of the log ionic conductivity with the inverse of temperature of the chitosan matrix and the chitosan$_n$[C_2mim][Dy(SCN)$_4$] membranes

Fig. 6 Photographs of the chitosan$_n$[C_2mim][Dy(SCN)$_4$] membranes

High ionic conductivity is one of the most important properties that a PE should fulfill. The chitosan$_1$[C_2mim][Dy(SCN)$_4$] membrane shows the highest ionic conductivity with 6.76×10^{-6} S·cm^{-1} at 30 °C and 5.62×10^{-4} S·cm^{-1} at 100 °C. On the opposite side, the chitosan$_{0.5}$[C_2mim][Dy(SCN)$_4$] membrane displays the lowest ionic conductivity in the analyzed temperature range. Generally, the ionic conductivity is expected to increase with the increase of the IL incorporated in the sample but, when we compared chitosan$_2$[C_2mim][Dy(SCN)$_4$] and chitosan$_4$[C_2mim][Dy(SCN)$_4$], the higher amount of IL (for n = 2) plays opposite effect. The ionic conductivity values decrease, which can be attributed to aggregation of ions, formation of clusters or undissolved IL. This is not corroborated by XRD data, but the SEM image for sample chitosan$_2$[C_2mim][Dy(SCN)$_4$] exhibit an irregular texture probably undissolved IL. At higher IL levels, there is a decrease of the free volume and available coordination sites which results in a decrease in conductivity values. Nevertheless, the ionic conductivity of a sample depends on several factors including the number, charge and mobility of the ionic species present in the PE [10]. The same exact lack of pattern, i.e., first the ionic conductivity decreases with the increase of the added IL, then it increases and finally it decreases again was also found by R. Alves et al [43] for membranes based on chitosan and dysprosium triflate. This paradigm shift probably results from the equilibrium between the formation of ionic aggregates and the increase/decrease of the free volume and available coordination sites.

Along with the aforesaid thermal, morphological and electrochemical properties these samples show a flexible nature and a transparent yellowish color. The yellow's intensity increases with the increase of added IL (Fig. 6). These characteristics are an advantage as they allow the application of these materials in see-through and/or flexible electrochemical devices.

Conclusions

The thermal (TGA and DSC), morphological (XRD, SEM and AFM) and electrochemical (ionic conductivity) properties of a new series of chitosan polymer electrolytes doped with different quantities of a dysprosium-based IL were evaluated. These polymer electrolytes, which were prepared through the solvent casting method, revealed interesting properties that might allow them to find application in practical electrochemical devices. They showed good thermal stability (T_{onset} > 139 °C), a predominantly amorphous morphology combined with the presence of small crystalline domains, and a satisfactory ionic conductivity (6.76×10^{-6} S·cm^{-1} at 30 °C and 5.62×10^{-4} S·cm^{-1} at 100 °C for the chitosan$_1$[C_2mim][Dy(SCN)$_4$ membrane). The characterization techniques showed that the crystalline domains are IL-related and that they are probably clusters of undissolved IL. These clusters might also have influenced the values of ionic conductivity, which did not follow a trend regarding the concentration of IL incorporated in the membranes. In summary, the results presented in the work encourage further studies for an optimization of these materials properties and future application in solid-state electrochemical devices.

Acknowledgments The financial support of the Brazilian agencies Capes and CNPq is gratefully acknowledged as well as the support by Fundação para a Ciência e a Tecnologia (FCT/MCTES) in the Strategic Funding grant UID/QUI/0686/2019 and in the framework of the Research unit Associate Laboratory for Green Chemistry- LAQV which is financed by national funds (UID/QUI/50006/2019), grant SRFH/BD/90366/2012 (R.L.), and two contracts under Investigador FCT program (IF/00355/2012 - J.M.S.S.E. and IF/00621/2015 - P.M.R.).

References

1. Earle MJ, Esperança JMSS, Gilea MA, Canongia Lopes JN, Rebelo LPN, Magee JW, Seddon KR, Widegren JA (2006) The distillation and volatility of ionic liquids. Nature 439:831–834
2. Smiglak M, Reichert WM, Holbrey JD, Wilkes JS, Sun LY, Thrasher JS, Kirichenko K, Singh S, Katritzky AR, Rogers RD (2006) Combustible ionic liquids by design: is laboratory safety another ionic liquid myth? Chem Commun 24:2554–2556
3. Baranyai KJ, Deacon GB, MacFarlane DR, Pringle JM, Scott JL (2004) Thermal degradation of ionic liquids at elevated temperatures. Aust J Chem 57:145–147
4. Ohno H (2005) Electrochemical aspects of ionic liquids. Wiley, USA
5. Plechkova NV, Seddon KR (2008) Applications of ionic liquids in the chemical industry. Chem Soc Rev 37:123–150
6. Holbrey JFD, Seddon KR (1999) Ionic liquids. Clean Prod Processes 1:223–236
7. Mallick B, Balke B, Felser C, Mudring A-V (2008) Dysprosium room-temperature ionic liquids with strong luminescence and response to magnetic fields. Angew Chem Int Ed 47:7635–7638

8. Arenz S, Babai A, Binnemans K, Driesen K, Giernoth R, Mudring A-V, Nockemann P (2005) Intense near-infrared luminescence of anhydrous lanthanide (III) iodides in an imidazolium ionic liquid. Chem Phys Lett 402:75–79
9. M.B. Armand, J.M. Chabagno, M.T. Duclot, Polymeric solid electrolytes in 'Proceeding of the Second International Meeting on Solid State Electrolytes, St. Andrews, Scotland' 6.5.1. (1978)
10. Gray FM (1991) Solid polymer electrolytes: fundamentals and technological applications. VCH, New York
11. Fernandes M, Nobre SS, Rodrigues LC, Gonçalves A, Rego R, Oliveira MC, Ferreira RAS, Fortunato E, Silva MM, Carlos LD, de Zea Bermudez V (2011) Li^{+}- and Eu^{3+}-doped poly(ε-caprolactone)/Siloxane biohybrid electrolytes for Electrochromic devices. ACS Appl Mater Interfaces 3:2953–2965
12. Pawlicka A, Danczuk M, Wieczorek W, Zygadlo-Monikowska E (2008) Influence of plasticizer type on the properties of polymer electrolytes based on chitosan. J Phys Chem A 112:8888–8895
13. Avellaneda CO, Vieira DF, Al-Kahlout A, Leite ER, Pawlicka A, Aegerter MA (2007) Solid-state electrochromic devices with Nb_2O_5:Mo thin film and gelatin-based electrolyte. Electrochim Acta 53:1648–1654
14. Machado GO, Ferreira HCA, Pawlicka A (2005) Influence of plasticizer contents on the properties of HEC based solid polymeric electrolytes. Electrochim Acta 50:3827–3831
15. Raphael E, Avellaneda CO, Manzolli B, Pawlicka A (2010) Agar-based films for application as polymer electrolytes. Electrochim Acta 55:1455–1459
16. Alves R, Donoso JP, Magon CJ, Silva IDA, Pawlicka A, Silva MM (2016) Solid polymer electrolytes based on chitosan and europium triflate. J Non-Cryst Solids 432:307–312
17. Leones R, Rodrigues LC, Pawlicka A, Esperança JMSS, Silva MM (2012) Characterization of flexible DNA films. Electrochem Commun 22:189–192
18. Leones R, Sentanin F, Rodrigues LC, Marrucho IM, Esperança JMSS, Pawlicka A, Silva MM (2012) Investigation of polymer electrolytes based on agar and ionic liquids. Express Polym Lett 6:1007–1016
19. Leones R, Sentanin F, Rodrigues LC, Ferreira RAS, Marrucho IM, Esperança JMSS, Pawlicka A, Carlos LD, Silva MM (2012) Novel polymer electrolytes based on gelatin and ionic liquids. Optical Mat 36:187–195
20. Leones R, Rodrigues LC, Fernandes M, Ferreira RAS, Cesarino I, Pawlicka A, Carlos LD, de Zea Bermudez V, Silva MM (2013) Electro-optical properties of the DNA-Eu^{3+} bio-membranes. J Electroanal Chem 708:116–123
21. Leones R, Fernandes M, Sentanin F, Cesarino I, Lima JF, de Zea Bermudez V, Pawlicka A, Magon CJ, Donoso JP, Silva MM (2014) Ionically conducting Er^{3+}-doped DNA-based biomembranes for electrochromic devices. Electrochim Acta 120:327–333
22. Leones R, Fernandes M, Ferreira RAS, Cesarino I, Lima JF, Carlos LD, Bermudez d Z, Magon CJ, Donoso JP, Silva MM, Pawlicka A (2014) Luminescent DNA and Agar-based membranes. J. Nanosci. Nanotechnol 14:6685–6691
23. Leones R, Botelho MBS, Sentanin F, Cesarino I, Pawlicka A, Camargo ASS, Silva MM (2014) Pectin-based polymer electrolytes with Ir(III) complexes. Mole Crys Liq Crys 604:117–125
24. Leones R, Esperança JMSS, Pawlicka A, Bermudez VD, Silva MM (2015) Polymer electrolyte based on DNA and N,N,N-trimethyl-N-(2-hydroxyethyl) ammonium bis(trifluoromethylsulfonyl) imide. J Electroanal Chem 748:70–75
25. Leones R, Sentanin F, Nunes SC, Esperança JMSS, Gonçalves MC, Pawlicka A, de Zea Bermudez V, Silva MM (2015) Effect of the alkyl chain length of the ionic liquid anion on polymer electrolytes properties. Electrochim Acta 184:171–178
26. Leones R, Sabadini RC, Esperança JMSS, Pawlicka A, Silva MM (2017) Playing with ionic liquids to uncover solid polymer electrolytes. Solid State Ionics 300:46–52
27. Leones R, Sabadini RC, Esperança JMSS, Pawlicka A, Silva MM (2017) Effect of storage time on the ionic conductivity of chitosan-solid polymer electrolytes incorporating cyano-based ionic liquids. Electrochim Acta 232:22–29
28. Leones R, Reis PM, Sabadini RC, Ravaro LP, Silva IDA, de Camargo ASS, Donoso JP, Magon CJ, Esperança JMSS, Pawlicka A, Silva MM (2017) A luminescente europium ionic liquid to improve the performance of chitosan polymer electrolytes. Electrochim Acta 240:474–485
29. Leones R, Sabadini RC, Sentanin FC, Esperança JMSS, Pawlicka A, Silva MM (2017) Polymer electrolytes for electrochromic devices through solvent casting and sol-gel routes. Sol Energy Mater Sol Cells 169:98–106
30. Ma J, Sahai Y (2013) Chitosan biopolymer for fuel cell applications. Carbohyd Polym 92:955–975
31. Pillai CKS, Paul W, Sharma CP (2009) Chitin and chitosan polymers: chemistry, solubility and fiber formation. Prog Polym Sci 34: 641–678
32. Hirano S, Seino H, Akiyama Y, Nonaka I (1990) Chitosan: a biocompatible material for oral and intravenous administrations. In: Gebelein CG (ed) Progress in biomedical polymers. Springer, New York, p 283
33. Dash M, Chiellini F, Ottenbrite RM, Chiellini E (2011) Chitosan-a versatile semisynthetic polymer in biomedical applications. Prog Polym Sci 36:981–1014
34. Gaf R (1992) Chitin chemistry. MacMillan Press Ltd, Houndmills
35. Rami L, Malaise S, Delmond S, Fricain JC, Siadous R, Schlaubitz S, Laurichesse E, Amedee J, Montembault A, David L, Bordenave L (2014) Physicochemical modulation of chitosan-based hydrogels induces different biological responses: interest for tissue engineering. J Biomed Mater Res A 102:3666–3676
36. Fuentes S, Retuert PJ, Gonzalez G (2003) Transparent conducting polymer electrolyte by addition of lithium to the molecular complex chitosan-poly(aminopropylsiloxane). Electrochim Acta 48:2015–2019
37. Yahya MZA, Arof AK (2003) Effect of oleic acid plasticizer on chitosan-lithium acetate solid polymer electrolytes. Eur Polym J 39:897–902
38. Morni NM, Arof AK (1999) Chitosan-lithium triflate electrolyte in secondary lithium cells. J Power Sources 77:42–48
39. Petrosyants S, Dobrokhotova Z, Ilyukhin A, Efimov N, Mikhlina Y, Novotortsev V (2015) Europium and terbium thiocyanates: syntheses, crystal structures, luminescence and magnetic properties. Inorg Chim Acta 434:41–50
40. Tang S, Babai A, Mudring A-V (2008) Europium-based ionic liquids as luminescent soft materials. Angew Chem Int Ed 47:7631–7634
41. Smith MJ, Silva CJ, Silva MM (1993) The study of a lanthanum triflate based polymer electrolyte using electrochemical and thermal techniques. Solid State Ionics 60:73–78
42. Pawlicka A, Sentanin F, Firmino A, Grote JG, Kajzar F, Rau I (2011) Ionically conducting DNA-based membranes for eletrochromic devices. Synth Met 161:2329–2334
43. Alves R, Sentanin F, Sabadini RC, Pawlicka A, Silva MM (2017) Solid polymer electrolytes based on chitosan and $Dy(CF_3SO_3)_3$ for electrochromic devices. Solid State Ionics 310:112–120